BUTTERWORTH HEINEMANN

Polymer Vol. 36 No. 9, pp. 1731–1741, 1995

0032-3861/95/$10.00 + 0.00

special section

The banded microstructure of sheared liquid-crystalline polymers*

Christopher Viney†‡§ and Wendy S. Putnam‡
†Molecular Bioengineering Program, Center for Bioengineering WD-12, and
‡Department of Materials Science and Engineering FB-10, University of Washington, Seattle, WA 98195, USA

It has been widely documented that nematic and cholesteric liquid-crystalline materials can develop a one-dimensionally periodic microstructure subsequent to uniaxial draw, unidirectional shear, or injection moulding. This microstructure gives rise to a banded texture between crossed polars. A review of the literature, which contains many conflicting studies, identified several molecular and processing variables that may affect the rate of banded texture evolution. Our research focused on banded textures in three lyotropic systems of hydroxypropyl cellulose (HPC), a semiflexible polymer: HPC–water, HPC–methanol and HPC–acetone. Solutions were sheared unidirectionally with a motorized parallel-plate apparatus. The rate of band evolution after shear was quantified consistently in terms of the time taken for the average band spacing to reach a minimum, and was found to depend on a combination of prior shear rate, specimen thickness, solvent type and concentration. The dependence on solvent type is especially sensitive. The qualitative way in which these variables control the rate of microstructural change after shear is discussed in terms of (1) their effect on the ability of a sheared microstructure to store the energy that drives subsequent reordering and (2) their effect on the mobility of the microstructure.

(Keywords: banded microstructure; liquid crystal; shear)

INTRODUCTION

Following thin-film shear[1,2], uniaxial fibre drawing[3], injection moulding[4], or elongational flow[5], nematic and cholesteric liquid-crystalline materials typically exhibit a one-dimensionally periodic microstructure. This is especially evident when thin specimens are observed between crossed polars. Dark bands lie perpendicular to the shear or flow direction Z, and are regularly spaced if Z is aligned parallel to the vibration direction of either polar. Detailed analysis of this microstructure[2,6–9] indicates that the global molecular alignment introduced by processing has partially relaxed, and that the local molecular orientation instead varies periodically relative to the macroscopic shear direction (*Figure 1*).

BACKGROUND

Motivation for studying banded textures

A polymer under load will extend more readily if the microstructure contains crimps, pleats or undulations that can be straightened, compared to the extension that is achieved if covalent backbone bonds are highly aligned along the direction of load. The serpentine and zig-zag microstructures in *Figure 1*, therefore, can be regarded as one-dimensional arrays of stiffness-reducing defects that substantially affect mechanical properties[10,11]. Efforts to optimize the mechanical properties of flow-processed (drawn, sheared or moulded) liquid-crystalline polymers require an understanding of the conditions under which banded textures are formed.

Significantly, we note two classes of stiff polymer that are produced from lyotropic solutions and do *not* exhibit banded textures:

(i) Kevlar 149 fibre has a tensile modulus of about 150 GPa[12], a 30% increase over the modulus of Kevlar 49. Unlike earlier versions of fibre drawn from lyotropic poly(*p*-phenylene terephthalamide), the higher-modulus material does not exhibit a banded microstructure[13].

(ii) Natural silk fibres (some of which exhibit strength and stiffness rivalling that of Kevlar 149) also do not exhibit a banded texture. However, a banded texture *is* present in silk fibres or films obtained when natural secretions are drawn or sheared by hand, which demonstrates that the defect is not intrinsic to liquid-crystalline molecular order, but is related to processing[14–16].

Ubiquitous nature of banded textures

Apart from the fact that banded textures form in response to a variety of flow geometries, they are common to both thermotropic and lyotropic liquid crystals, and to both macromolecular and small-molecule systems. Indeed, they were initially described in the context of films consisting of soaps[17] or small-molecule nematic dyes[18]. The bands can appear during continuous shear[1,19], or after cessation of shear[20,21]. In either case,

* Presented at 'Aspects of Imaging in Polymer Science', 51st Annual Meeting of the Microscopy Society of America, 1–6 August 1993, Cincinnati, OH, USA

§To whom correspondence should be addressed. Present address: Department of Materials, University of Oxford, Parks Road, Oxford OX1 3PH, UK

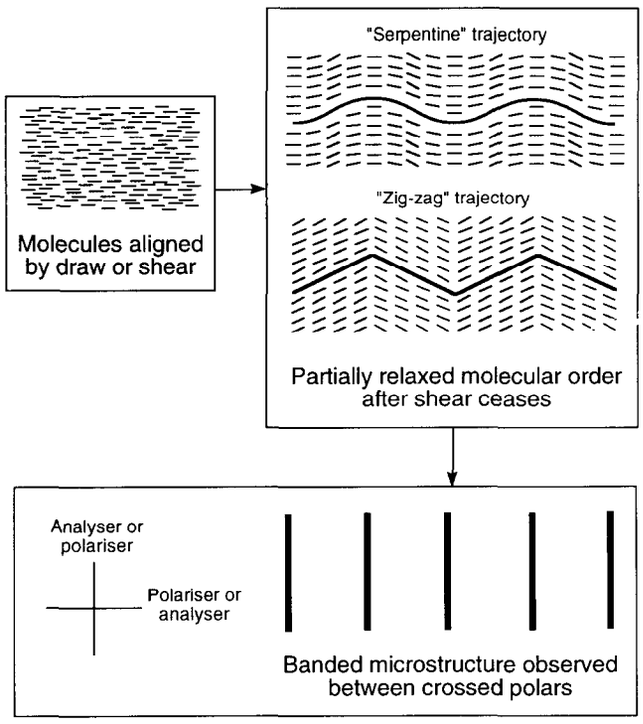

Figure 1 Schematic representation of molecular order that gives rise to a banded microstructure between crossed polars

a critical deformation rate must be exceeded[1,19–24]; this condition can be predicted theoretically[25]. A finite time must elapse from the onset of shear[1] or the cessation of shear[21,23] before the bands can form.

A similar microstructure is observed when previously aligned liquid-crystalline polymers are exposed to appropriately oriented magnetic fields[26,27] or thermal gradients[28]. The macroscopic similarity of banded textures in these different cases suggests that they may be caused by related processes at the molecular level.

Why banded textures form

A simple model describes a mechanism for how a one-dimensional periodic microstructure can result from application of a *magnetic* field[29]. Consider the case of a nematic film mechanically aligned along the z direction, which also corresponds to the magnetic director. A magnetic field $\boldsymbol{H}$ is applied in the plane of the sample and perpendicular to z. Above a threshold field $\boldsymbol{H}_c$, the director will reorient parallel to $\boldsymbol{H}$. The perturbation in the molecular orientation grows exponentially at a rate inversely proportional to the effective viscosity of the reorientation process. If the director rotates uniformly in the plane of the sample, the process does not generate shear flow, and the process is limited by purely rotational viscosity. For a rod-like polymer, the relatively large rotational viscosity results in a slow uniform reorientation process. If, instead, the director responds in a spatially periodic manner, shear flows characterized by viscosities lower than the pure rotational viscosity will be generated in the sample. Since the effective viscosity of the periodic response is lower than that of the uniform process, the periodic response develops at a faster initial rate, suppressing the slower uniform response. The periodic response leads to an observable banded texture.

A similar mechanism has been deduced experimentally for banded textures that result from mechanical shear[21,30,31]. In this case, an *internal* driving force exists for band evolution. The shear deformation promotes molecular alignment; however, this alignment is disrupted by disclinations in the sample. At low shear rates, it is observed that the flow distorts the defects but cannot significantly rearrange them, and no special optical textures appear upon cessation of shear. At higher shear rates, the molecules become significantly oriented; the defects become highly localized while the rest of the fluid contains oriented molecules and a low density of defects. (Also, it has recently been observed that shear can transiently generate disclinations of higher strength than those found in equilibrium microstructures[32].) The Frank elastic energy stored in the defects provides the driving force to reorient the director (*Figure 2*), thus reducing the overall distortion energy without significant loss of *local* nematic order. The kinetics of reorientation are modified by interaction between the specimen and its bounding surfaces[33–35].

Previous characterization by microscopy

The molecular order responsible for banded textures has been studied extensively by various techniques of light microscopy[1–3,6–9,11,19–23,36–51], transmission electron microscopy[2,6,8,33–35,37,39,52–56] and scanning electron microscopy[4,13,39,40,42–44,46,47,54]. The light microscopy studies include imaging in polarized light[1–3,6–9,11,19–23,36–51] and under phase-contrast conditions[38], and observation of optical diffraction patterns in the objective back focal plane[2,3,8,38,51].

The band spacing often approaches the limits of light-optical resolution, which, coupled with the one-dimensional character of the microstructures, can lead to some otherwise unusual image artifacts[57]. Even if there is no question about the banded texture being resolved properly, light microscopy may not necessarily be an accurate indicator of how the angle of molecular misorientation (relative to the shear direction) varies as a function of position measured along the shear direction. This problem can occur because the extinction directions that are observed between crossed polars depend locally on the orientation of the polarizability tensor, and, if the local symmetry of molecular order is sufficiently low, the

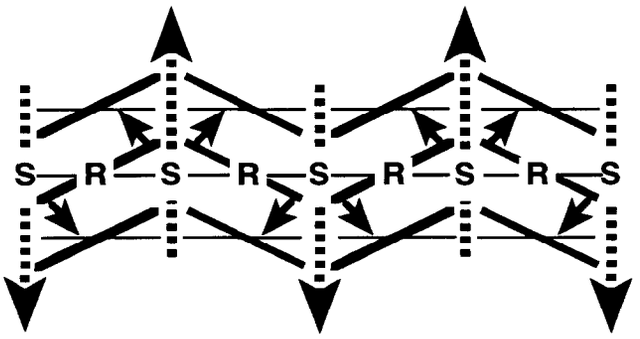

Figure 2 Evolution of banded texture. Shear flows (S) are associated with fluctuations that localize the dominant director rotation (R) in periodic domains. Local order is preserved, while global order relaxes. Initial, shear-induced director orientation is horizontal, indicated by thin solid lines. Director orientations after partial relaxation are indicated by thick solid lines

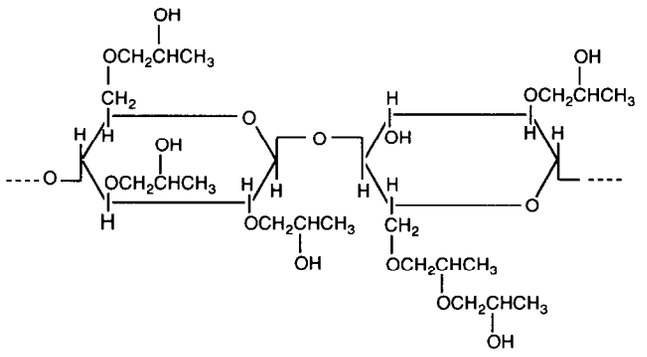

Figure 3 Idealized chemical structure of hydroxypropyl cellulose. The segment as shown has an average degree of substitution equal to 3

principal axes of this tensor need not correspond in any straightforward way to the local direction of molecular orientation[6,58]. Electron microdiffraction[6], or electron microscopy of fracture surfaces[43], etched samples[44,46,47] or decorated samples[59], can unambiguously reveal the molecular trajectory relative to the shear direction. The lack of simple correspondence between extinction directions and molecular axes is exhibited by thermotropic main-chain polymers that contain phenyl groups and can therefore assemble into domains that exhibit the necessary optical biaxiality[6,58].

The banded texture in hydroxypropyl cellulose (HPC)

HPC (*Figure 3*) has served as the '*Drosophila*' for experimentation on banded textures[5,7,11,19,21–23,31,36,37,40,42,45,48,49,60,61]. It is popular as a model compound for these studies because it is inexpensive and non-toxic, it forms lyotropic solutions in a variety of common solvents at room temperature, and it also[62] behaves thermotropically. Furthermore, the bands are relatively coarse, and thus (1) they are easily resolved by light microscopy even when a long-working-distance objective with limited numerical aperture is used to accommodate a shearing stage, and (2) image artifacts associated with fine microstructures are greatly reduced[57]. Finally, the molecular structure of HPC does not promote assembly into optically biaxial domains, so the molecular trajectory relative to the shear direction *can* be deduced from observations made between crossed polars. A significant shortcoming of HPC in banded texture studies is that the molecules are semiflexible, and cannot therefore be realistically described as hard rods. This severely limits the extent to which experimental results can be compared with the predictions of current theoretical models. Also, while current models are developed for nematic liquid crystals, the molecular order in lyotropic HPC is cholesteric; nematic order can be reasonably assumed during and immediately after shear, but not in the later stages of post-shear relaxation.

Both zig-zag (sharply kinked)[7,40,42] and serpentine (smooth)[63] molecular trajectories (*Figure 1*) have been reported for banded HPC specimens. One study[45] suggests a zig-zag trajectory, with a serpentine path replacing the apex of the zig-zag. From combined optical and electron microscopy, it has been deduced that the trajectory has an out-of-plane component[42,45].

Effect of molecular and processing variables on HPC banded textures

The development of banded textures in HPC solutions depends on several molecular parameters and processing conditions: polymer molecular weight, shear rate, sample thickness, type of solvent, solution concentration, duration of shear and method of applying shear. It is also possible that degree of substitution (hydroxypropylation) may have an effect, though this parameter is difficult to quantify accurately. At the same time, there are various ways in which one might attempt to characterize the banded texture and its development: for example, time elapsed between cessation of shear and development of bands (induction time; measurement is subjective), length of time over which banded texture persists (relaxation time; subjective), band spacing (changes with time; objective) and maximum divergence angle between molecular trajectory and shear direction (also changes with time; objective). The literature on banded textures contains many attempts to correlate change in a parameter describing a banded texture with change in a molecular characteristic or processing condition. Unfortunately, because there are so many variables, it is rarely possible to compare the observations made in different studies, and the literature contains many conflicting results. Also, theory is not sufficiently developed to suggest which microstructural parameter will be most sensitive to changes in any given molecular or processing parameter, and anticipated correlations frequently cannot be demonstrated conclusively.

Reported values of the band spacing in aqueous HPC solutions range from 4 to 10 μm[21,23]. Light diffraction experiments (on specimens sheared mechanically between parallel glass plates) showed that the band spacing is relatively insensitive to shear rate and sample thickness, while increasing the solution concentration decreases the spacing[60]. Another study (performed on samples sheared by hand between a glass slide and coverslip) reported that the band spacing increases with increasing concentration[63]. An attempt to correlate band spacing to molecular persistence length[64] did not reveal any trends.

A banded texture will not form unless the magnitude of shear and the shear rate exceed threshold values. The critical magnitude of shear is a decreasing function of the shear rate[21–23]. There is disagreement as to whether the critical magnitude of shear does[22] or does not[21,23] depend on sample thickness. In the case where a thickness dependence was observed[22], thicker samples favoured band formation. For aqueous HPC solutions, the critical shear rate is nearly independent of polymer concentration over the 40–60 wt% range[21,23]. Conflicting data have been reported on whether critical shear rate is increased[23] or decreased[21] by increasing polymer molecular weight.

The induction and relaxation times of band formation decrease as the prior shear rate increases[19,21,23]. Also, these timescales increase with increasing HPC molecular weight[21]. These observations are consistent with the qualitative mechanism described above for banded texture formation.

EXPERIMENTAL

We sought to investigate systematically the effect of several variables (shear rate, specimen thickness, solvent

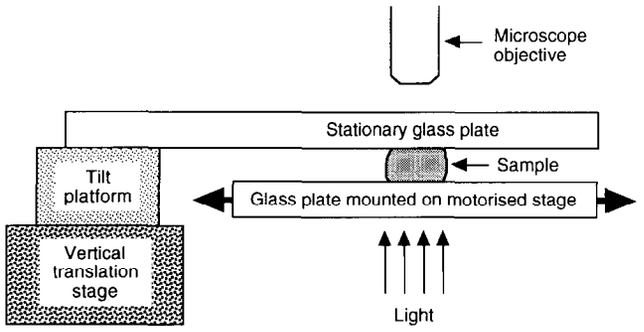

Figure 4 Schematic representation of microscope stage modified to shear samples unidirectionally between parallel glass plates

type and concentration) on banded texture formation under controlled conditions. The shear rates that we used were higher than those quoted by previous investigators[21,23,63], and therefore better approximate actual fibre-drawing and film-forming processes.

Materials and sample preparation

HPC (tradename Klucel E) was provided in the form of a dry powder by Aqualon (Wilmington, DE). The typical weight-average molecular weight of this material is 80 000[65], and the degree of substitution is approximately 3.45 hydroxypropyl groups per anhydroglucose unit[66].

Solutions of Klucel E were prepared in the following solvents: water, methanol and acetone. The solubility parameters[67] of these solvents are 23.4, 14.5 and 9.9 $(\text{cal cm}^{-3})^{1/2}$, respectively. This suggests that water is relatively the best solvent for HPC and acetone is relatively the poorest, since HPC is more soluble in polar solvents[65]. For each system, solutions were prepared at concentrations of 37, 45, 53 and 61 wt% polymer. These concentrations were chosen to lie within the isotropic (37 wt%), biphasic (45 wt%) and anisotropic (53 and 61 wt%) regions of the HPC–water phase diagram; the lower and upper concentration limits of biphasic separation at room temperature have been quoted as 40–42 and 47–50 wt% for weight-average molecular weights in the range 80 000 to 100 000[68,69]. The literature did not provide sufficient information concerning phase separation in the methanol or acetone solutions, so polarized light microscopy was used to determine whether the solutions in these solvents were isotropic, biphasic, or anisotropic.

Solutions were prepared at room temperature by slowly adding dry HPC powder to the solvent while stirring. Because HPC tends to form a sticky, inhomogeneous paste when large amounts are added to solvent, we initially prepared dilute solutions. Solutions were then concentrated by evaporation until the solution mass equalled the amount corresponding to the desired concentration. In cases where a significant amount of polymer adhered to the side of the container as solvent evaporated, the sample vial was immersed in a heated water bath, and small additional amounts of solvent were periodically used to flush the adhering material into the bulk solution[70]. Solutions were allowed to homogenize in sealed vials for at least one week prior to use.

Shearing stage

Experiments were conducted with a parallel-plate apparatus, fitted to a Leitz Laborlux 12 POL transmitted polarized light microscope[71,72] (*Figure 4*). The device provides controlled shear of a sample between two glass plates, a stationary upper plate and a motorized lower plate. The experimental arrangement ensures that the velocity gradient is the same in every vertical column of material in the field of view (unlike the situation between rotating parallel discs), and the thickness is also constant (unlike the situation in cup-and-cone geometries). However, we are limited to applying shear in a given direction for only a (short) finite length of time.

The upper plate is cantilevered from a Newport model 37 tilt platform, which in turn is attached to a Newport model 415 translation stage that permits vertical positioning of the upper plate with an accuracy of 0.5 μm. Because the upper plate is cantilevered, the plate separation is expected to decrease from left to right across the field of view. However, by using beam theory and the properties of plate glass to calculate the deflection[70], it was determined that the resultant difference in sample thickness across the field of view is insignificant compared to the $\pm 5\,\mu$m roughness of the plate glass as measured by surface profilometry.

The lower plate is attached to a motorized Leitz model 1089 x–y stage. Joystick control provides two plate velocities of 9.05 and 2.45 cm s^{-1}. All shears involved displacing the lower plate horizontally through a distance of 2 cm.

Parallelism of the glass plates was obtained as follows. A machinist's level with a sensitivity of 0.05 mm/m was placed along two perpendicular directions on the lower plate to determine its plane. The level was then placed on the upper plate, and the two micrometers on the tilt platform were adjusted to align the upper plate with the lower one.

Two values of sample thickness were used: 50 and 100 μm. The smaller value represents the minimum thickness that we consider to be acceptable, given the unevenness of the glass surfaces. (We decided against polishing the surfaces to optical flatness, to avoid the possibility of introducing directionality.) To obtain images in acceptable focus, we were constrained to sample thicknesses $\leqslant 100\,\mu$m. The choice of sample thicknesses, and the available velocities of the motorized stage, gives shear rates in the range 245 to 1810 s^{-1}. The plate separation was fixed by the following procedure. The microscope was focused (through the upper plate, and with no sample present) on the top surface of the lower plate. The fine-focus adjustment, which bears a scale calibrated in increments of 2 μm, was used to lower the microscope stage by a known amount D. The bottom surface of the upper plate was then brought into focus by adjusting the micrometer on its vertical translation stage, and the micrometer setting for the plate separation D was recorded. Subsequent loading of the sample was performed by raising the upper plate, depositing solution on the lower plate, and promptly lowering the upper plate to the predetermined micrometer setting. Thus, during and after shear, the microscope remains focused on the top surface of the specimen, which provides the clearest images of the banded microstructures. To minimize solvent evaporation during our observations, we applied vacuum grease around the edges of the plates

after shearing. Experiments were repeated to ensure reproducibility.

Recording microstructures

Micrographs were recorded with a Canon T-90 camera, equipped with a Command Back 90 to enable automated exposures at fixed time intervals. To 'freeze' the microstructural relaxation and so minimize blurring, high-speed film (Fuji Neopan 1600 ASA) was used.

Characterizing microstructural change

To determine the effect of molecular and processing variables on the rate at which banded textures form, it is necessary to identify a criterion that quantitatively samples a consistent stage of band development. Attempts to use either the time at which bands first appear or at which they disappear are too subjective; evolution of the microstructure is a continuous process, and the microstructure retains evidence of periodicity for some time after the initially straight bands have degenerated into wavy lines (*Figures 5* and *6*). Instead, by quantifying the average band periodicity as a function of time elapsed since cessation of shear, we found that the periodicity consistently passes through a minimum (*Figure 7*). The minimum band spacing occurs at some time after the banded texture appears to be most clearly developed. By studying a series of photographs of the evolving banded texture, we noted that the bands appeared to break up after the average band spacing had reached a minimum. Also, the time to reach an arbitrary increase in band spacing (e.g. 10%) above the minimum consistently followed the same trends as the time to reach the minimum band spacing. Spacing data were not collected in experiments where the combination of molecular and process variables gave poorly defined banded textures.

Data for the plots of average band spacing *versus* time (e.g. *Figure 7*) were collected as follows. Micrographs showing the banded texture at known times after cessation of shear were printed at a total magnification of 900×. At least five horizontal lines were drawn through randomly selected areas of each micrograph, parallel to the shear direction. The distance between 21 extinction bands was measured carefully along each line. From this distance, an average band spacing over 20 band intervals was calculated. The values calculated from each line were then averaged to obtain the mean band spacing quoted from the micrograph (constituting a single data point on the plot of band spacing *versus* time), and their standard deviation was used to define an error bar. To determine the position of the minimum for a particular experiment, the data close to the minimum were fitted to a parabola (using Cricket Graph Version 1.3.2). The equation of the parabola was then used to calculate the value of the minimum band spacing and the time after shear when the minimum occurred.

As an alternative method for determining average band spacing, a Bertrand lens can be used to observe the objective back focal plane; the spacing between diffracted orders is inversely proportional to the real band spacing[2,3,8,38,51]. However, the typically diffuse nature of the diffracted orders precludes an accurate measurement of their separation.

RESULTS AND DISCUSSION

Solutions that form a banded texture

One objective of this study was to determine whether specimens must be liquid-crystalline in order for bands to form. *Table 1* indicates whether our solutions prior to shear were isotropic, biphasic, or anisotropic, as determined by polarized light microscopy.

Klucel E–acetone solutions. The 37 wt% (isotropic), 45 wt% (isotropic) and 53 wt% (anisotropic) acetone solutions did not form a distinct banded texture, for shear rates up to $1810\,s^{-1}$. Banded textures formed in the 61 wt% (anisotropic) acetone solutions for each of the shear rates that we investigated. Studies[21] of Klucel E–*water* solutions have demonstrated that shearing must efficiently orient molecules if a banded texture is to form subsequently. We suggest that the polymer molecules are difficult to orient globally in the acetone solutions because acetone is not a thermodynamically good solvent for HPC.

Klucel E–methanol solutions. Bands did not form in 37 wt% (isotropic) or 45 wt% (biphasic) solutions at shear rates up to $1810\,s^{-1}$.

In contrast to the behaviour of the solutions in acetone, bands were formed by *both* of the fully anisotropic solutions (53 and 61 wt% polymer) in methanol (*Table 1*). Because methanol is thermodynamically a better solvent than acetone for HPC, one can expect a greater degree of *intrinsic* extension and alignment in the methanol-based solutions. Also, because methanol and acetone have approximately the same density ($0.79\,g\,cm^{-3}$ to two significant figures[73]), *Table 1* suggests that the methanol-based solutions require a smaller volume fraction of polymer to form a liquid-crystalline phase, compared to the acetone-based solutions. As the critical volume fraction required for mesophase formation is predicted to decrease with increasing Kuhn segment length[74,75], the observed phase behaviour is consistent with the methanol-based solutions having a greater degree of chain extension and alignment.

Klucel E–water solutions. We noted above that water is thermodynamically better than methanol as a solvent for HPC. Again, banded textures did not form after shearing the 37 wt% (isotropic) or 45 wt% (biphasic) solutions at shear rates up to $1810\,s^{-1}$. These results are consistent with previous work[21] reporting that a shear rate exceeding $100\,s^{-1}$ could not induce bands in isotropic or biphasic solutions of Klucel E (weight-average molecular weights 60 000 and 100 000) in water. However, the present results contradict a report[63] that 45 wt% Klucel E–water solutions form bands after shearing at a rate of approximately $20\,s^{-1}$. We believe that concentration control (by means of vacuum grease applied around the edges of the glass plates after shearing) was more successful in the present set of experiments.

Banded textures could be induced in the 53 and 61 wt% Klucel E–water solutions, which were fully anisotropic. Continuous observation of the 53 wt% solution confirmed that the banded texture began to evolve only *after* cessation of shear. These results are consistent with previous studies of HPC[21].

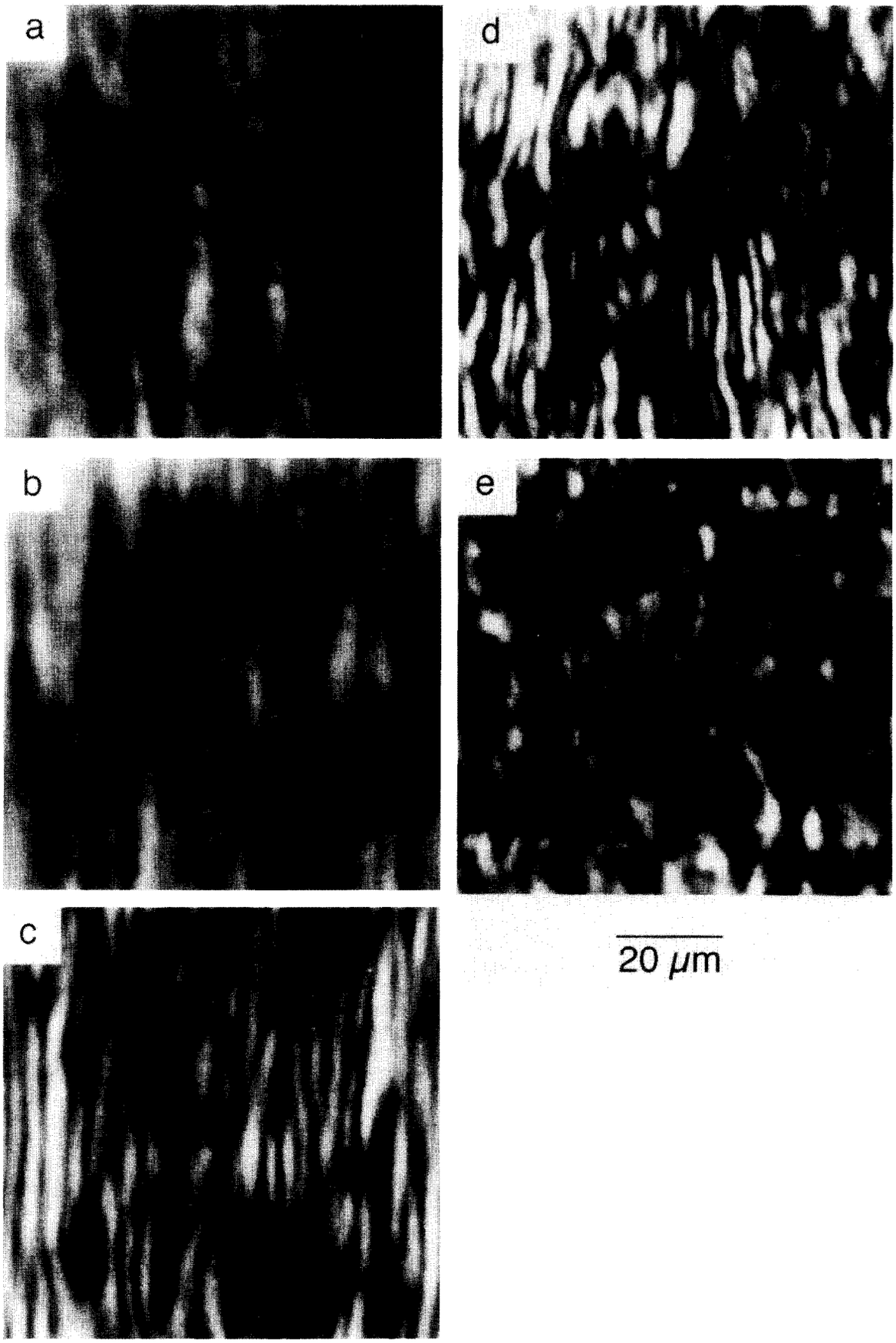

Figure 5 Evolution of banded texture in 61 wt% Klucel E–acetone solution, after shear at 245 s^{-1}. Specimen thickness is 100 μm; the shear direction is horizontal. The time elapsed after shear ceased is (a) 1.10 min, (b) 10.08 min, (c) 20.07 min, (d) 50.17 min, (e) 70.15 min. A Microtek ScanMaker 600ZS scanner and Adobe Photoshop image processing software were used to generate the composite image from individual printed micrographs

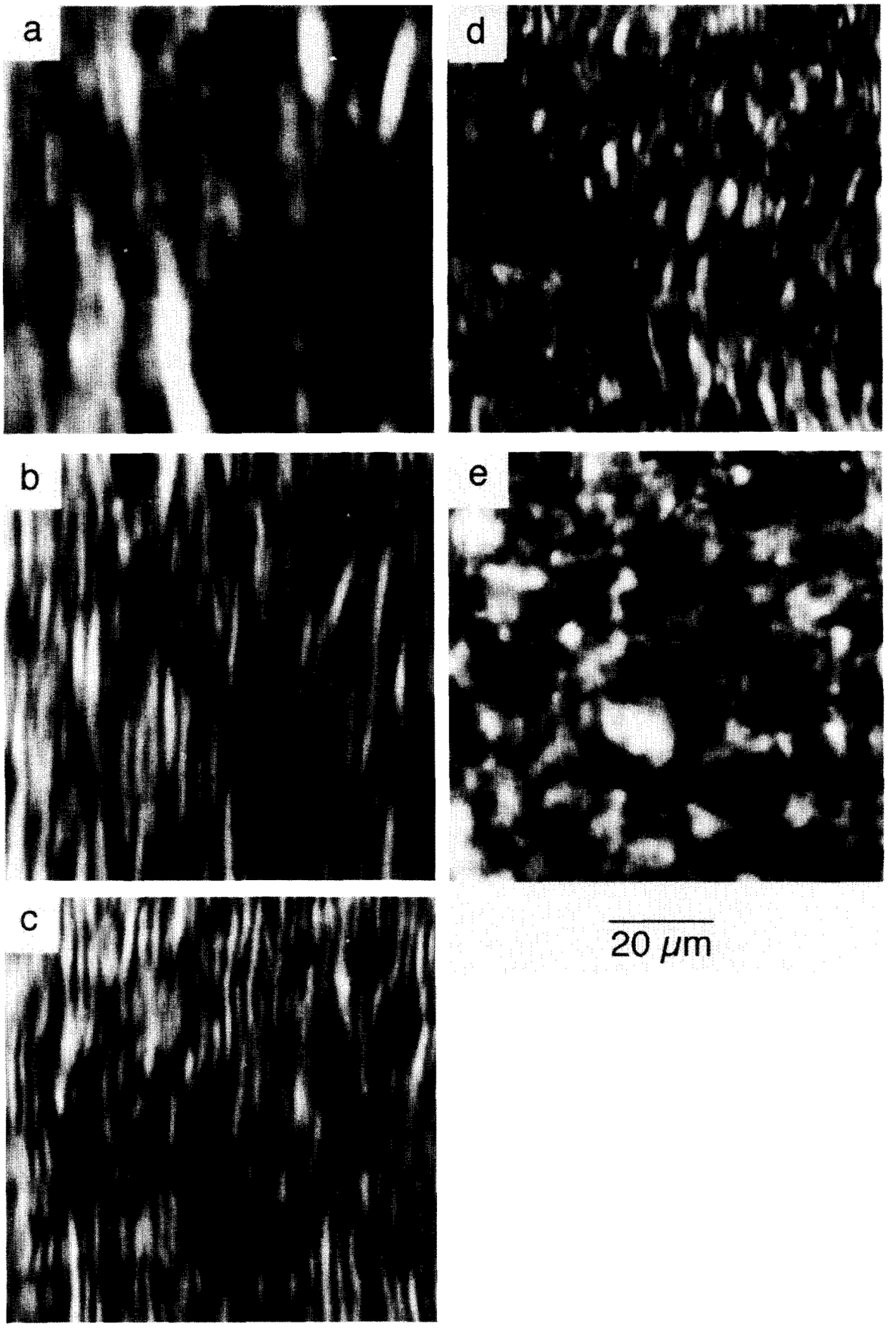

Figure 6 Evolution of banded texture in 53 wt% Klucel E–water solution, after shear at 490 s^{-1}. Specimen thickness is 100 μm; the shear direction is horizontal. The time elapsed after shear ceased is (a) 7 s, (b) 17 s, (c) 47 s, (d) 77 s, (e) 117 s. A Microtek ScanMaker 600ZS scanner and Adobe Photoshop image processing software were used to generate the composite image from individual printed micrographs

Rate of banded texture evolution

For a variety of experimental conditions, *Table 2* lists values of the time elapsed between cessation of shear and banded textures attaining their minimum periodicity. Spacing data were not collected from several experiments conducted with samples of 100 μm thickness, because well defined banded textures did not develop. For the same reason, spacing data were not obtained from the 53 wt% Klucel E–acetone solutions.

Effect of shear rate. A shear-rate dependence was observed in the Klucel E–acetone solutions, as shown in *Figure 7* and *Table 2* (entries 3 and 4); the band evolution time was shorter at the higher shear rate. No significant dependence of microstructural evolution on shear rate was observed in the case of Klucel E–methanol (*Table 2*, entries 6 and 7) or Klucel E–water solutions (*Table 2*, entries 9 and 11). The last observation is consistent with previous work on specimens sheared between parallel glass plates[60]. However, it stands in contrast to a study[21] (conducted in a cone-and-plate geometry at shear rates less than $20\,s^{-1}$, i.e. substantially lower than ours) that showed Klucel E–water to behave in a qualitatively similar fashion to our Klucel E–acetone solutions.

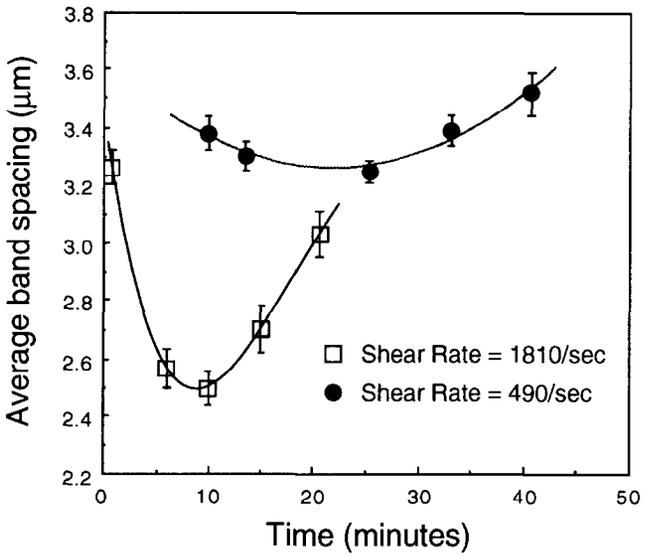

Figure 7 Band spacing as a function of time after cessation of shear, for 61 wt% Klucel E–acetone solutions. Specimen thickness is 50 μm

Table 1 Phase behaviour of Klucel E solutions

	Concentration (wt%)			
Solvent	37	45	53	61
Acetone	Isotropic	Isotropic	Anisotropic	Anisotropic
Methanol	Isotropic	Biphasic	Anisotropic	Anisotropic
Water	Isotropic	Biphasic	Anisotropic	Anisotropic

This set of results can also be understood in terms of the previously discussed need for shear to generate a microstructure that provides the necessary internal driving force for relaxation to a banded texture. If an increase in shear rate generates a microstructure that stores more internal energy to drive relaxation, a shorter band evolution time should result. In the case of HPC–acetone (poor solvent; global molecular alignment more difficult to achieve), the shear rate of $1810\,s^{-1}$ is still within this regime. In the case of HPC–methanol or HPC–water (better solvents; global molecular alignment more easily achieved), even the shear rate of $490\,s^{-1}$ is sufficient to saturate the internal driving force for subsequent relaxation.

Effect of thickness. In *Table 2*, the different shear rates in entries 9 and 11 were obtained by changing the velocity of the upper glass plate; the similar microstructural mobilities observed subsequent to cessation of shear have already been noted. However, the rate of banded texture evolution is significantly more rapid after shear at an intermediate rate obtained by changing the *thickness* of an otherwise identical sample (entry 10). On this basis, we deduce that samples of different thickness, but subjected to identical shear rates by also varying the relative velocities of the bounding surfaces, will exhibit different rates of banded texture evolution. We suggest that the observed thickness effect reflects the constraining effect of the glass plates, which can more effectively retard bulk molecular rearrangement in thinner samples.

Previous experiments have given conflicting results. By focusing at different levels in a sample, various investigators observed the evolution of banded textures under conditions of variable thickness. Although no change in

Table 2 Band development times

Entry No.	System	Conc. (wt%)	Shear rate (s^{-1})	Thickness (μm)	Development time
1	Klucel E–acetone	53	490	Bands not fully developed	
2		61	245	100	39 min
3		61	490	50	22 min
4		61	1810	50	9 min
5	Klucel E–methanol	53	490	50	9 s
6		61	490	50	15 s
7		61	1810	50	17 s
8	Klucel E–water	53	490	50	55 s
9		61	490	50	43 s
10		61	905	100	32 s
11		61	1810	50	42 s

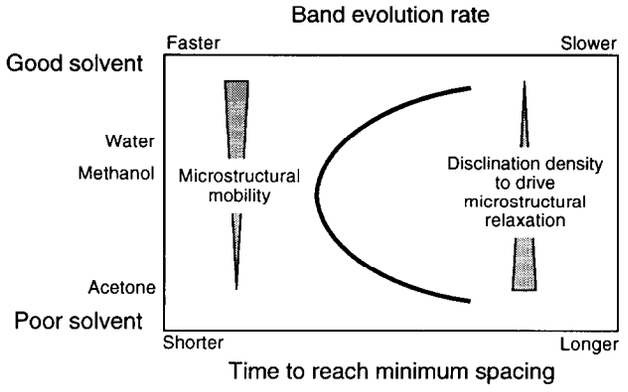

Figure 8 Schematic representation of competing solvent-related effects that govern the rate of banded microstructure formation

the texture at different levels was reported in two studies conducted in a cone-and-plate geometry[21,23], a third study, conducted on specimens between parallel plates, found that bands did not develop uniformly throughout the sample thickness[22]. As in the previous section, we recognize that experimental observations of banded texture formation are sensitive to the geometry in which shear is generated. Because our results obtained with parallel plates indicate that plate velocity and specimen thickness can have different effects on subsequent microstructural evolution, we encourage other investigators to perform their studies under conditions where these variables can be studied independently.

Effect of solvent. *Table 2* shows that banded texture evolution is significantly more sluggish in HPC–acetone than in HPC–water or HPC–methanol. Since acetone is thermodynamically the least good solvent, we expect that polymer chains in the acetone solutions will have the most disordered equilibrium conformation, and therefore the highest probability of entanglement. A high degree of entanglement translates to reduced molecular mobility, and lower rates of microstructural change. However, based on this simplistic argument, we should expect the rate of microstructural evolution to be greatest in the water-based solutions, i.e. in the thermodynamically best solvent. Instead, *Table 2* shows that the bands evolve most quickly in the methanol-based solutions, so the contribution of additional factors to the rate of microstructure evolution must be considered.

We noted in an earlier section that the evolution of banded textures is driven by elastic energy temporarily stored in defects that have been multiplied and localized during shear. Thus, the rate of microstructural evolution after shear must depend on the amount of energy that is stored in such defects. A given energy per unit volume can be stored either in a smaller number of higher-energy disclinations or in a larger number of lower-energy disclinations. The latter situation is more effective at promoting subsequent microstructural rearrangement, because there are more disclination pairs to interact and redistribute through the microstructure. The distortion energy per unit length of disclination is directly proportional[76] to the magnitude of the splay, twist and bend elastic constants (k_{11}, k_{22} and k_{33} respectively). For rigid rods (a necessary oversimplification in the present case), the elastic constants can be quantified in terms of the following combination of parameters[77,78]:

$$k_{ii} = C\phi^2 L^4 DkT$$

where ϕ is the rod concentration, L and D respectively are the length and diameter of the rods, k is Boltzmann's constant, T is the absolute temperature and C is a constant for a given orientation distribution of the rods. For semiflexible molecules, L does not correspond directly to the chain length; an appropriate statistical length, such as the Kuhn segment length, must be used instead. Therefore, L will be greater in a thermodynamically better solvent. Conditions that favour larger values of L (and therefore of k_{ii}) will lead to a microstructure that contains *fewer* defects per unit volume immediately after shear.

The rate at which banded textures are observed to evolve can now be interpreted qualitatively in terms of driving and resisting forces:

(i) The stored energy available to drive post-shear microstructural change should be distributed over the greatest number of disclinations in HPC–acetone (poorest solvent, smallest L) systems, and over the smallest number of disclinations in HPC–water (best solvent, largest L) systems. Thus the sheared HPC–acetone solutions should be the most susceptible (and the HPC–water solutions should be the least susceptible) to subsequent microstructural rearrangement, if the microstructural mobilities were comparable in both cases.

(ii) The ability of the microstructure to respond to the driving force for change is least in HPC–acetone (poorest solvent, greatest entanglement) systems, and greatest in HPC–water (best solvent, least entanglement) systems. These relative mobilities are consistent with qualitative observations of solution viscosities, which for comparable concentrations are highest for solutions in acetone and lowest for solutions in water.

In HPC–methanol, both the available driving force and microstructural mobility lie between these extremes, and combine to give the fastest rate of band evolution (*Figure 8*).

Effect of concentration. A measure of the polymer conformation in a solvent is given by the coefficient a in the Mark–Houwink equation:

$$[\eta] = kM^a$$

where $[\eta]$ is the intrinsic viscosity of the polymer solution, M is the viscosity-average polymer molecular weight, and k and a are constants for a particular polymer–solvent system at a given temperature. The value of a varies from 0.5 for random coils to 2 for rigid rods[79]. A value of $a \sim 0.9$ has been estimated[80] for HPC chains in dilute aqueous solutions; this value indicates that the chains are far from being in a fully extended conformation at low concentrations. The likelihood of chains being in extended conformations increases with concentration in the liquid-crystalline state. A synergism of increasing chain extension and cooperative alignment, as a function of increasing concentration in the liquid-crystalline state, has been described previously for semiflexible lyotropic and thermotropic polymers[81]. These concepts may explain the more rapid rate of band evolution in 61 wt% Klucel E–water solutions, compared to the rate in 53 wt%

solutions (*Table 2*, entries 8 and 9): molecules in a more highly oriented, extended state are less likely to entangle. Therefore, even though there are more chains per unit volume, microstructural rearrangements should occur more rapidly at higher concentrations, as observed.

The opposite trend is exhibited by the Klucel E–methanol solutions: the average band spacing reaches a minimum more slowly in the 61 wt% solution than it does in the 53 wt% solution (*Table 2*, entries 5 and 6). Since methanol is a thermodynamically less good solvent than water for HPC, the polymer chains will have an even less extended conformation than those in an aqueous solution, favouring chain entanglement. If the viscosity decrease associated with enhanced chain extension and alignment at higher concentrations cannot offset the viscosity increase associated with there being more chains per unit volume, slower rates of microstructural change will result.

CONCLUSIONS

The following conclusions are drawn for solutions of HPC (a semiflexible polymer) subjected to shear between parallel plates:

Isotropic and biphasic solutions in acetone, methanol and water do not form banded microstructures, even after shearing for 2 cm at a rate of $1810\,s^{-1}$. Anisotropic solutions form banded microstructures if the rate of prior shear is sufficiently high.

The rate of band evolution after shear can be usefully characterized in terms of the time taken to reach the minimum average band spacing.

The rate at which the global molecular orientation relaxes after shear depends on a combination of prior shear rate, specimen thickness, solvent type and concentration. The dependence on solvent type is especially sensitive.

The timescale of band evolution is longest in the Klucel E–acetone solutions. Bands take minutes to form in the acetone solutions and seconds to form in the Klucel E–water and Klucel E–methanol solutions. Band evolution rates are governed by a trade-off between the effects of solvent on (a) microstructural mobility (chain entanglement, viscosity) and (b) the disclination density that stores the energy available to drive post-shear microstructural change.

In the Klucel E–water system, band evolution occurs more slowly in a 53 wt% solution than in a 61 wt% solution. The opposite trend is observed in the Klucel E–methanol system. This difference can be explained qualitatively in terms of how polymer–solvent interactions affect chain conformation and entanglement.

ACKNOWLEDGEMENTS

This work was supported by the College of Engineering at the University of Washington, the American Chemical Society (Petroleum Research Fund, Grant No. 21300–G7), the IBM Corporation, and a fellowship (to WSP) from the DuPont Company. Aqualon Company (Wilmington, DE) kindly donated Klucel samples.

REFERENCES

1 Kiss, G. and Porter, R. S. *Mol. Cryst. Liq. Cryst.* 1980, **60**, 267
2 Donald, A. M., Viney, C. and Windle, A. H. *Polymer* 1983, **24**, 155
3 Simmens, S. C. and Hearle, J. W. S. *J. Polym. Sci., Polym. Phys. Edn.* 1980, **18**, 871
4 Thapar, H. and Bevis, M. *J. Mater. Sci. Lett.* 1983, **2**, 733
5 Peuvrel, E. and Navard, P. *Macromolecules* 1991, **24**, 5683
6 Viney, C., Donald, A. M. and Windle, A. H. *Polymer* 1985, **26**, 870
7 Horio, M., Ishikawa, S. and Oda, K. *J. Appl. Polym. Sci., Appl. Polym. Symp.* 1985, **41**, 269
8 Viney, C. and Windle, A. H. *Polymer* 1986, **27**, 1325
9 Navard, P. and Zachariades, A. E. *J. Polym. Sci. (B) Polym. Phys.* 1987, **25**, 1089
10 Allen, S. R. and Roche, E. J. *Polymer* 1989, **30**, 996
11 Wang, J. and Labes, M. M. *Macromolecules* 1992, **25**, 5790
12 Roche, E. J., Allen, S. R., Fincher, C. R. and Paulson, C. *Mol. Cryst. Liq. Cryst.* 1987, **153**, 547
13 Krause, S. J., Vezie, D. L. and Adams, W. W. *Polym. Commun.* 1989, **30**, 10
14 Kerkam, K., Viney, C., Kaplan, D. L. and Lombardi, S. J. *Nature* 1991, **349**, 596
15 Kerkam, K., Kaplan, D. L., Lombardi, S. J. and Viney, C. in 'Materials Synthesis Based on Biological Processes' (Eds. M. Alper, P. D. Calvert, R. Frankel, P. C. Rieke and D. A. Tirrell), Materials Research Society, Pittsburgh, 1991, p. 239
16 Viney, C., Huber, A. and Verdugo, P. in 'Biodegradable Polymers and Packaging' (Eds. C. Ching, D. L. Kaplan and E. L. Thomas), Technomic, Lancaster, PA, 1993, p. 209
17 Rosevear, F. B. *J. Soc. Cosmetic Chem.* 1968, **19**, 581
18 Dreyer, J. F. in 'Liquid Crystals and Ordered Fluids' (Eds. J. F. Johnson and R. S. Porter), Plenum, New York, 1970, p. 311
19 Navard, P. *J. Polym. Sci., Polym. Phys. Edn.* 1986, **24**, 435
20 Alderman, N. J. and Mackley, M. R. *Faraday Discuss. Chem. Soc.* 1985, **79**, 149
21 Ernst, B. and Navard, P. *Macromolecules* 1989, **22**, 1419
22 Marrucci, G., Grizzuti, N. and Buonaurio, A. *Mol. Cryst. Liq. Cryst.* 1987, **153**, 263
23 Marsano, E., Carpaneto, L. and Ciferri, A. *Mol. Cryst. Liq. Cryst.* 1988, **158(B)**, 267
24 Takebe, T., Hashimoto, T., Ernst, B., Navard, P. and Stein, R. S. *J. Chem. Phys.* 1990, **92**, 1386
25 Zielinska, B. J. A. and ten Bosch, A. *Phys. Rev. (A)* 1988, **38**, 5465
26 Rose, D. V. and Kuzma, M. R. *Mol. Cryst. Liq. Cryst. Lett.* 1986, **4**, 39
27 Rey, A. D. and Denn, M. M. *Liq. Cryst.* 1989, **4**, 409
28 Palangana, A. J., Depeyrot, J. and Figueiredo Neto, A. M. *Phys. Rev. Lett.* 1990, **65**, 2800
29 Lonberg, F., Fraden, S., Hurd, A. J. and Meyer, R. E. *Phys. Rev. Lett.* 1984, **52**, 1903
30 Maffettone, P. L., Grizzuti, N. and Marrucci, G. *Liq. Cryst.* 1989, **4**, 385
31 Ernst, B., Navard, P., Hashimoto, T. and Takebe, T. *Macromolecules* 1990, **23**, 1370
32 Viney, C., Brown, D. J., Dannels, C. M. and Twieg, R. J. *Liq. Cryst.* 1993, **13**, 95
33 Donald, A. M. *J. Mater. Sci. Lett.* 1984, **3**, 44
34 Donald, A. M. and Windle, A. H. *J. Mater. Sci.* 1984, **19**, 2085
35 Donald, A. M. and Windle, A. H. *Polymer* 1984, **25**, 1235
36 Onogi, Y., White, J. L. and Fellers, J. F. *J. Non-Newtonian Fluid Mech.* 1980, **7**, 121
37 Atkins, E. D. T., Fulton, W. S. and Miles, M. J. in 5th Int. Dissolving Pulps Conf. (TAPPI), Vienna, 1980, p. 208
38 Viney, C., Donald, A. M. and Windle, A. H. *J. Mater. Sci.* 1983, **18**, 1136
39 Zachariades, A. E. and Logan, J. A. *Polym. Eng. Sci.* 1983, **23**, 797
40 Shimamura, K. *Makromol. Chem., Rapid Commun.* 1983, **4**, 107
41 Zachariades, A. E., Navard, P. and Logan, J. A. *Mol. Cryst. Liq. Cryst.* 1984, **110**, 93
42 Nishio, Y. and Takahashi, T. *J. Macromol. Sci.–Phys. (B)* 1984–85, **23**, 483
43 Hu, S., Xu, M., Li, J., Qian, B., Wang, X. and Lenz, R. W. *J. Polym. Sci., Polym. Phys. Edn.* 1985, **23**, 2387
44 Chen, S., Jin, Y., Hu, S. and Xu, M. *Polym. Commun.* 1987, **28**, 208
45 Fried, F. and Sixou, P. *Mol. Cryst. Liq. Cryst.* 1988, **158(B)**, 163
46 Windle, A. H., Dong, Y., Lemmon, T. J. and Spontak, R. J. in 'Frontiers of Macromolecular Science' (Eds. T. Saegusa, T. Higashimura and A. Abe), Blackwell, Oxford, 1989, p. 343

47 Bedford, S. E. and Windle, A. H. *Polymer* 1990, **31**, 616
48 Peuvrel, E. and Navard. P. *Liq. Cryst.* 1990, **7**, 95
49 Gleeson, J. T., Larson, R. G., Mead, D. W., Kiss, G. and Cladis, P. E. *Liq. Cryst.* 1992, **11**, 341
50 Larson, R. G. and Mead, D. W. *Liq. Cryst.* 1992, **12**, 751
51 Picken, S. J., Moldenaers, P., Berghmans, S. and Mewis, J. *Macromolecules* 1992, **25**, 4759
52 Dobb, M. G., Johnson, D. J. and Saville, B. P. *J. Polym. Sci., Polym. Symp.* 1977, **58**, 237
53 Dobb, M. G., Johnson, D. J. and Saville, B. P. *J. Polym. Sci., Polym. Phys. Edn.* 1977, **15**, 2201
54 Li, L.-S., Allard, L. F. and Bigelow, W. C. *J. Macromol. Sci.–Phys (B)* 1983, **22**, 269
55 Thomas, E. L. and Wood, B. A. *Faraday Discuss. Chem. Soc.* 1985, **79**, 229
56 Donald, A. M. *Polym. Commun.* 1986, **27**, 18
57 Viney, C. and Windle, A. H. *Phil. Mag. (A)* 1987, **55**, 463
58 Viney, C., Mitchell, G. R. and Windle, A. H. *Mol. Cryst. Liq. Cryst.* 1985, **129**, 75
59 Spontak, R. J., Personal Communication, 1993
60 Fincher, Jr, C. R. *Mol. Cryst. Liq. Cryst.* 1988, **155**, 559
61 Guido, S., Grizzuti, N. and Marrucci, G. *Liq. Cryst.* 1990, **7**, 279
62 Shimamura, K., White, J. L. and Fellers, J. F. *J. Appl. Polym. Sci.* 1981, **26**, 2165
63 Donald, A. M., Viney, C. and Ritter, A. P. *Liq. Cryst.* 1986, **1**, 287
64 Marsano, E., Personal Communication, 1990
65 Aqualon Company (Wilmington, DE) product literature 'Klucel Hydroxypropylcellulose: Physical and Chemical Properties', 1987
66 Taylor, S. (Aqualon Company), Personal Communication, 1990
67 Grulke, E. in 'Polymer Handbook', 1st Edn. (Eds. J. Brandrup and E. H. Immergut), Wiley, New York, 1966, p. IV–347
68 Fried, F. and Sixou, P. *J. Polym. Sci., Polym. Chem. Edn.* 1984, **22**, 239
69 Onogi, Y., White, J. L. and Fellers, J. F. *J. Polym. Sci., Polym. Phys. Edn.* 1980, **18**, 663
70 Putnam, W. S., Master's Thesis, University of Washington, Seattle, 1990
71 Putnam, W. S. and Viney, C. in 'Electron Microscopy 1990: XIIth Int. Congr. for Electron Microscopy', San Francisco Press, San Francisco, CA, 1990, p. 1092
72 Putnam, W. S. and Viney, C. *Mol. Cryst. Liq. Cryst.* 1991, **199**, 189
73 Weast, R. C. (Ed.) 'Handbook of Chemistry and Physics', 64th Edn., CRC Press, Boca Raton, FL, 1983
74 Gray, D. G. *J. Appl. Polym. Sci., Appl. Polym. Symp.* 1983, **37**, 179
75 Flory, P. J. *Adv. Polym. Sci.* 1984, **59**, 1
76 de Gennes, P. G. 'The Physics of Liquid Crystals', Oxford University Press, Oxford, 1979
77 Straley, J. P. *Phys. Rev. (A)* 1973, **8**, 2181
78 DuPré, D. B. in 'Polymer Liquid Crystals' (Eds. A. Ciferri, W. R. Krigbaum and R. B. Meyer), Academic Press, New York, 1982, p. 165
79 Sperling, L. H. 'Introduction to Physical Polymer Science', 1st Edn., Wiley, New York, 1986
80 Werbowyj, R. S. and Gray, D. G. *Macromolecules* 1980, **13**, 69
81 Viney, C., Yoon, D. Y., Reck, B. and Ringsdorf, H. *Macromolecules* 1989, **22**, 4088